Available online at www.sciencedirect.com
ScienceDirect
European Journal of Mechanics B/Fluids 27 (2008) 750–770

Supercritical surface gravity waves generated by a positive forcing

J.W. Choi [a], S.M. Sun [b,*], S.I. Whang [c]

[a] *Department of Mathematics, Korea University, Seoul, Korea*
[b] *Department of Mathematics, Virginia Polytechnic Institute and State University, Blacksburg, VA, USA*
[c] *National Institute of Mathematical Science, Daejun, Korea*

Received 23 May 2007; received in revised form 13 January 2008; accepted 21 January 2008

Available online 20 February 2008

Abstract

Forced surface waves on an incompressible, inviscid fluid in a two-dimensional channel with a small bump on a horizontal rigid flat bottom are studied. The wave motion on the free surface is determined by a nondimensional wave speed F, called Froude number, and $F = 1$ is a critical value of F. If $F = 1 + \lambda\epsilon$ with $\epsilon > 0$ a small parameter, then a time-dependent forced Korteweg–de Vries (FKdV) equation can be derived to model the wave motion on the free surface. Here, the case $\lambda \geqslant 0$ (or $F \geqslant 1$, called supercritical case) is considered. The steady FKdV equation is first studied both theoretically and numerically. It is shown that there exists a cut-off value λ_0 of λ. For $\lambda \geqslant \lambda_0$ there are steady solutions, while for $0 \leqslant \lambda < \lambda_0$ no steady solution of FKdV exists. For the unsteady FKdV equation, it is found that for $\lambda > \lambda_0$, the solution of FKdV with zero initial condition tends to a stable steady solution, whilst for $0 < \lambda < \lambda_0$ a succession of solitary waves are periodically generated and continuously propagating upstream as time evolves. Moreover, the solutions of FKdV equation with nonzero initial conditions are studied.

Keywords: Supercritical surface waves; Forced gravity waves

1. Introduction

Forced surface waves in a two-dimensional fluid flow have attracted much attention in last thirty years. The fluid of finite depth is assumed to be incompressible, inviscid and bounded above by a free surface and below by a rigid bottom, which has a small bump on an otherwise flat bottom. Let the depth of fluid at infinity be a constant h and the speed of the flow far upstream be a constant C. The wave motion on the free surface is determined by a nondimensional wave speed, called Froude number F and defined by $F = C/\sqrt{gh}$, where g is the gravity constant. It is well-known that F has a critical value $F = 1$ near which the linear theory of the problem is not valid and nonlinear theory must be developed [25]. The surface wave is called supercritical (subcritical) if $F > 1$ ($F < 1$). Such surface waves over a flat bottom (no bump) were first studied by J. Scott Russell [23] experimentally and later by Boussinesq [3–6], Rayleigh [22], and Korteweg and de Vries [18] from a balance of dispersive and nonlinear effects. After nondimensionalizing the problem, a formal model equation

$$\eta_t - (1/3)\eta_{xxx} - 3\eta\eta_x + 2\lambda\eta_x = 0, \quad x \in (-\infty, +\infty),\ t > 0. \tag{1.1}$$

* Corresponding author.
E-mail address: sun@math.vt.edu (S.M. Sun).

0997-7546/$ – see front matter
doi:10.1016/j.euromechflu.2008.01.006

called Korteweg–de Vries (KdV) equation, can be derived to approximate solutions of the exact equations governing the fluid motion, where $F = 1 + \lambda\epsilon$ with $\epsilon > 0$ small, $h(1 + \epsilon\eta(\epsilon^{1/2}hx, \epsilon\sqrt{h/g}\,t))$ is the function for the free surface, and x, t are nondimensional horizontal and time variables, respectively. Moreover, it is straightforward to show that besides the trivial solution $\eta = 0$, for $c < 2\lambda$, (1.1) has nontrivial traveling-wave solutions

$$S_{c,x_0}(x) = (2\lambda - c)\,\mathrm{sech}^2\big(\sqrt{3(2\lambda - c)}(x - x_0 - ct)/2\big)$$

that approach to zero exponentially at infinity. If $c = 0$, then λ must be positive, which corresponds to the supercritical case ($F > 1$). In this paper, we only consider surface waves generated by a small bump on a flat bottom with $\lambda > 0$.

Steady (time-independent) waves over a semicircular bump on a flat bottom were first studied numerically by Forbes and Schwartz [14] and later by Vanden Broeck [28] and Forbes [13] using the exact governing equations. For supercritical cases, it was found that there is a cut-off value $F_0 > 1$ such that there are two branches of supercritical solutions when $F > F_0$, and no solutions when $1 < F < F_0$. Such supercritical solutions behave like solitary waves. As the size of the bump tends to zero, the solutions on one branch approach to the zero solution while the solutions on the other branch approach to the solitary wave solutions of the exact equations.

When $F = 1 + \epsilon\lambda$ with $\epsilon > 0$ a small parameter, a model equation

$$\eta_t - (1/3)\eta_{xxx} - 3\eta\eta_x + 2\lambda\eta_x = b_x, \quad x \in (-\infty, +\infty),\ t > 0, \tag{1.2}$$

called forced KdV (FKdV) equation, can be derived, where $b(x)$ is a nondimensional function related to the bump on the flat bottom. The solutions of the steady FKdV equation,

$$-(1/3)\eta_{xxx} - 3\eta\eta_x + 2\lambda\eta_x = b_x, \quad x \in (-\infty, +\infty), \tag{1.3}$$

were first studied in [24] for steady surface waves over a semicircular bump. It was shown that for supercritical cases, there is a cut-off value $\lambda_0 > 0$ of λ such that there are two branches of numerical solutions for $\lambda > \lambda_0$ and no solutions exist for $0 < \lambda < \lambda_0$. The solutions of the FKdV equation were then compared with the numerical solutions obtained in [28,13] and they agreed very well. The solutions of (1.3) were also discussed by Miles [21] for an impulse forcing $b(x) = \delta(x)$ and cusped solitary-wave solutions were found explicitly. Other steady surface waves for two-fluid flows were discussed in [12,10,15,9].

The time-dependent forced surface waves were first numerically investigated by Wu and Wu [30] using a generalized Boussinesq system. It was found that in supercritical cases with zero initial condition, a succession of solitary waves are periodically generated and continuously propagating ahead of the bump in procession, while a train of weakly dispersive waves develop behind the bump. This phenomenon was then studied experimentally in [19]. Similar results were obtained by Akylas [1], Cole [11] and Mei [20] based upon the time-dependent FKdV equation (1.2) with a singular or other forcing functions, while Grimshaw and Smyth [16] studied this problem using the modulation theory. Furthermore, stability results of the FKdV equation were derived for some steady solutions of the FKdV equation when the forcing term $b(x)$ was chosen as one of special sech^2- or sech^4-functions [7,8].

The purpose of this paper is to reconsider steady and unsteady solutions of the FKdV equation (1.2) theoretically and numerically. Assume that the function $b(x)$ is even in x and $\lambda \geqslant 0$ is the only parameter that varies. First, we consider the solutions of steady equation (1.3). It is rigorously proved that for each $\lambda > 0$ large, there exist two symmetric (i.e., even in x) solutions, η_s and η_ℓ, of (1.3), where η_s is near zero and η_ℓ is near the symmetric solitary wave solution $S(x) = S_{0,0}(x)$ of the corresponding homogeneous equation for (1.3). Any solution of (1.3) near zero is unique and must be symmetric. These solutions decay to zero exponentially at infinity. For $\lambda > 0$ small, there are no solutions (symmetric or asymmetric) of (1.3) that tend to zero at infinity. Then, it is shown numerically that there exists a cut-off value λ_0 such that for $\lambda > \lambda_0$ there exist exactly two branches of symmetric solutions of (1.3). As λ becomes large, one branch, which corresponds to η_ℓ, approaches to the solitary wave solution $S(x)$ and another branch, which corresponds to η_s, tends to zero. For $\lambda < \lambda_0$, there are no symmetric solutions of (1.3). Therefore, the numerical result is consistent with the theoretical result.

For time-dependent equation (1.2), we consider the initial value problem (IVP) of (1.2) with an initial condition

$$\eta(x, 0) = \eta_0(x). \tag{1.4}$$

The global well-posedness of the IVP in Sobolev space $H^1(R)$ is discussed using recent development of the IVP of the KdV equation (1.1). If $\eta_0 \in H^1(R)$, then there is a unique solution $\eta(x, t)$ defined in $H^1(R)$ for all $t > 0$ and the solution continuously depends on the initial condition $\eta_0(x)$ in $H^1(R)$. Moreover, we prove that if $\lambda > \sqrt{(3/2)\max|b(x)|}$,

the solution $\eta_s(x)$ of (1.3) is stable (in the Lyaponov sense) in the function space $H^1(R)$. Numerically, it is found that η_s is stable and η_ℓ is unstable under nonzero perturbations. Similar numerical stability results were also obtained in [29,15], where the numerical noise was taken as the perturbation. The solution of (1.2) with zero initial condition is then numerically calculated using a semi-circular bump. It is found that when $\lambda \geqslant \lambda_0$, the solution tends to $\eta_s(x)$ of (1.3) as $t \to \infty$. For $0 < \lambda < \lambda_0$, a succession of solitary waves are generated periodically and propagating continuously upstream with a constant speed, which were also found in [1,11,20,29]. Furthermore, we obtain that when λ is less than λ_0 and near λ_0, the time period T that is needed to generate one upstream solitary wave becomes very large and as $\lambda \to \lambda_0^-$, $T \to \infty$, which explains partly why there are no solitary waves generated for $\lambda \geqslant \lambda_0$. For nonzero initial conditions, we choose traveling solitary-wave solutions or two-soliton solutions initially placed far ahead or behind of the bump and moving towards the bump. It is found that there is a critical traveling speed of these initial solitary waves. When the speed of a traveling solitary wave is less than the critical speed, the result of the interaction between the solitary wave and the bump is that the solitary wave bounces back from the bump with changes of its traveling speed and amplitude. When the initial traveling speed is lager than the critical speed, the solitary wave passes over the bump with again changes of the traveling speed and amplitude. Moreover, after the interaction, there are always some dispersive waves developing either ahead or behind the bump and moving quickly to the infinity. For two-soliton waves as the initial data, if one has a traveling speed greater than the critical speed and another one has a speed less than the critical value, the two-soliton wave splits into two solitary waves, one bouncing back from the bump and another one passing over the bump. Therefore, in this case, the bump may act as a filtering mechanism to block slow-moving solitary waves. It is noted that these phenomena have not been discussed in literatures.

The paper is organized as follows. Section 2 briefly discusses the physical background of (1.2) and the ideas for the derivation of the equation. In Section 3, solutions of the steady equation (1.3) are discussed theoretically and numerically. Section 4 mainly concerns the time-dependent equation (1.2) with initial condition (1.4) and gives theoretical and numerical results for the solutions of the initial value problem.

2. Formulation

The problem considered here concerns two-dimensional surface waves on a fluid flow of constant density. The fluid is inviscid and incompressible, and bounded above by a free surface and below by an obstruction of compact support over a rigid horizontal bottom (Fig. 1). If the Cartesian coordinates (x^*, z^*) are chosen such that x^* is the horizontal variable and z^* is vertical variable, then the equations and boundary conditions governing the fluid motion are the following [25]:

$$u^*_{x^*} + w^*_{z^*} = 0,$$
$$u^*_{t^*} + u^* u^*_{x^*} + w^* u^*_{z^*} = -\frac{p^*_{x^*}}{\rho^*},$$
$$w^*_{t^*} + u^* w^*_{x^*} + w^* w^*_{z^*} = -\frac{p^*_{z^*}}{\rho^*} - g;$$

at the free surface $z^* = \eta^*$,

$$\eta^*_{t^*} + u^* \eta^*_{x^*} - w^* = 0,$$
$$p^* = 0;$$

at the rigid boundaries $z^* = H^*(x^*)$,

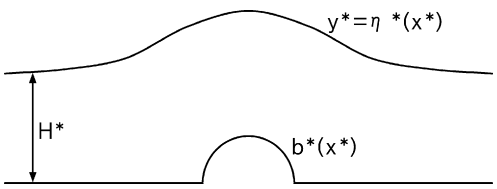

Fig. 1. Fluid domain.

$$w^* - u^* H^*_{x^*} = 0;$$

as $x^* \to -\infty$,

$$(u^*, w^*) \to (C, 0),$$

where (u^*, w^*) is the velocity vector, $y^* = \eta^*(x^*, t)$ is the equation of the free surface, ρ^* is the constant density of the fluid, g is the gravitational acceleration constant, p^* is the pressure, and $H^*(x^*) = -h + b^*(x^*)$. Here, h is the constant depth of the fluid at far upstream, and $b^*(x^*)$ stands for the obstruction with finite support on the rigid horizontal bottom.

To nondimensionalize the problem, we use the following dimensionless variables:

$$\epsilon^{1/2} = (h/L), \quad (x, z) = (\epsilon^{1/2} x^*/h, z^*/h), \quad (\tilde{u}, \tilde{w}) = (u^*, \epsilon^{-1/2} w^*)/\sqrt{gh},$$
$$\tilde{p} = p^*/(gh\rho^*), \quad \tilde{\eta} = \eta^*/h, \quad b(x) = b^*(x^*)/(h\epsilon^2), \quad t = \epsilon\sqrt{g/h}\, t^*,$$

where L is the horizontal length scale.

Let us assume that $\tilde{u}$, $\tilde{w}$, $\tilde{p}$, and $\tilde{\eta}$ have the following asymptotic expansions,

$$\phi(x, z, \epsilon) = \phi_0 + \epsilon\phi_1 + \epsilon^2\phi_2 + \epsilon^3\phi_3 + \mathrm{O}(\epsilon^4),$$

with $\tilde{u}_0 = 1$, $\tilde{w}_0 = 0$, $\tilde{p}_0 = -z + 1$ and $\tilde{\eta}_0 = 0$. The nondimensional upstream flow speed, called Froude number, is defined by $F = C/(gh)^{1/2} = 1 + \epsilon\lambda$. By substituting above asymptotic expansions into the nondimensionalized equations and boundary conditions and comparing the orders of ϵ, a sequence of equations and boundary conditions for the successive approximations are obtained according to the order of ϵ. Then, by solving the resulting equations with the assumptions $\tilde{\eta}(-\infty, t) = \tilde{\eta}_x(-\infty, t) = 0$, the forced Korteweg–de Vries (FKdV) equation (1.2) is obtained (for the sake of convenience, denote $\eta = \tilde{\eta}_1$). The detailed derivation can be found in [24].

3. Steady FKdV equation

In this section, we consider the time-independent FKdV equation (1.3) and its solutions that tend to zero at infinity. Integrating (1.3) from $-\infty$ to x, we obtain

$$-(1/3)\eta_{xx} - (3/2)\eta^2 + 2\lambda\eta = b(x). \tag{3.1}$$

In the following, we assume that $b(x)$ is even in x and compactly supported.

3.1. Existence of steady solutions for large $\lambda > 0$

If $b = 0$ and $\lambda > 0$, which corresponds to the supercritical case ($F > 1$), there are two symmetric solutions of (3.1): $\eta \equiv 0$ and

$$S(x) = 2\lambda \operatorname{sech}^2\big[(6\lambda)^{1/2} x/2\big]. \tag{3.2}$$

Now, we show that for nonzero $b(x)$ and each $\lambda > 0$ large, there exist two symmetric solutions of (3.1), one near zero and one near $S(x)$. First, define the space $C(R)$ as a space of continuous functions with maximum norm $\|f\| = \max_{x\in R} |f(x)|$.

Proposition 3.1. *If $\lambda > \sqrt{3\|b(x)\|/2}$, there is a unique solution $\eta_s(x)$ of (3.1) such that $\|\eta_s(x)\| \leqslant \sqrt{2\|b(x)\|/3}$. Moreover, $\eta_s(x)$ is symmetric in x.*

Proof. By using the Green's function for the linear operator of the left side of (3.1), we transform (3.1) into an integral form

$$\eta = \frac{1}{2\sqrt{6\lambda}} \int_{-\infty}^{\infty} e^{-\sqrt{6\lambda}|x-s|}\big((9/2)\eta^2(s) + 3b(s)\big)\,\mathrm{d}s := \mathcal{L}_0\eta, \tag{3.3}$$

where $b(x)$ is compacted supported. Define a closed ball $B = \{f(x) \in C(R) \mid \|f\| \leqslant r\}$ with $r = \sqrt{2\|b\|/3}$. For $\lambda > \sqrt{3\|b\|/2} = (3r/2)$, we have

$$\begin{aligned}\|\mathcal{L}_0\eta\| &\leqslant \frac{1}{2\sqrt{6\lambda}}\left\|\int_{-\infty}^{\infty} e^{-\sqrt{6\lambda}|x-s|}\left(\frac{9r^2}{2}+3\big|b(s)\big|\right)\mathrm{d}s\right\| \\ &\leqslant \frac{1}{2\sqrt{6\lambda}}\left(\frac{9r^2}{2}+3\big\|b(x)\big\|\right)\left\|\int_{-\infty}^{\infty} e^{-\sqrt{6\lambda}|x-s|}\,\mathrm{d}s\right\| \\ &\leqslant \frac{1}{12\lambda}\big(9r^2+6\big\|b(x)\big\|\big) \leqslant r\end{aligned}$$

and

$$\begin{aligned}\|\mathcal{L}_0\eta_1 - \mathcal{L}_0\eta_2\| &\leqslant \frac{1}{2\sqrt{6\lambda}}\left\|\int_{-\infty}^{\infty} e^{-\sqrt{6\lambda}|x-s|}\frac{9}{2}\big|\eta_1^2(s)-\eta_2^2(s)\big|\,\mathrm{d}s\right\| \\ &\leqslant \frac{9}{4\sqrt{6\lambda}}\left\|\int_{-\infty}^{\infty} e^{-\sqrt{6\lambda}|x-s|}2r\big|\eta_1(s)-\eta_2(s)\big|\,\mathrm{d}s\right\| \\ &\leqslant \frac{3r}{2\lambda}\big\|\eta_1(x)-\eta_2(x)\big\|,\end{aligned}$$

where $(3r/2\lambda) < 1$. Thus, the operator $\mathcal{L}_0$ is a contraction in B and by the contraction mapping theorem, there is a unique solution $\eta_s(x)$ of (3.1) satisfying $\max_{x\in R}|\eta_s(x)| \leqslant r$. Furthermore, if we define the set B for symmetric functions only, by using above argument, we can also show that there is a unique symmetric solution of (3.1). Thus, by the uniqueness, the solution $\eta_s(x)$ must be symmetric. □

Next, we show that for large $\lambda > 0$ there exists a unique symmetric solution η_ℓ of (3.1) near $S(x)$.

Proposition 3.2. *There is a $\tilde{\lambda}_0 > 0$ and $r > 0$ such that for $\lambda > \tilde{\lambda}_0$, there exists a unique symmetric solution $\eta_\ell(x)$ of* (3.1) *satisfying $\|\eta_\ell(x) - S(x)\| \leqslant r$.*

Proof. Write the solution of (3.1) as

$$\eta(x) = S(x) + u(x) \tag{3.4}$$

where $u(x)$ satisfies

$$-(1/3)u_{xx} - 3S(x)u - (3/2)u^2 + 2\lambda u = b$$

or

$$-u_{xx} - 9S(x)u + 6\lambda u = (9/2)u^2 + 3b. \tag{3.5}$$

It is easy to see that $u_1(x) = S'(x)$ is a solution of (3.5) when the right side is equal to zero. By using the Liouville formula, another linearly independent solution $u_2(x)$ can be found with the properties that $u_2(x)$ is symmetric in x and approaches to infinity with an order $\mathrm{O}(e^{\sqrt{6\lambda}|x|})$ as $|x| \to \infty$ (see [26]). Also, $u_1(x)$ and $u_2(x)$ satisfy

$$\big|u_1(x)u_2(s)\big| \leqslant \tilde{C}\lambda^{-1/2}\exp\big(-\sqrt{6\lambda}\,|x-s|\big) \tag{3.6}$$

where $\tilde{C}$ is a constant independent of x, s and λ. Thus, the symmetric solution of (3.5) can be written as

$$u = u_1(x)\int_0^x u_2(s)\big((9/2)u^2(s)+3b(s)\big)\,\mathrm{d}s + u_2(x)\int_x^{\infty} u_1(s)\big((9/2)u^2(s)+3b(s)\big)\,\mathrm{d}s := \mathcal{L}_1 u. \tag{3.7}$$

By choosing a closed ball $B = \{f(x) \in C(R) \mid \|f\| \leqslant r,\ f(x) = f(-x)\}$ with r small enough and $\lambda > 0$ large enough, we can use (3.6) and the similar argument in the proof of Proposition 3.1 to show that the operator $\mathcal{L}_1$ is a contraction in B. Hence, by the contraction mapping theorem, there is a $\tilde{\lambda}_0 > 0$ such that for $\lambda > \tilde{\lambda}_0$, there exists a unique solution $u(x)$ of (3.7) with $\|u(x)\| \leqslant r$. Therefore, for $\lambda > \tilde{\lambda}_0$, there is a unique symmetric solution η_ℓ of (3.1) with $\|\eta_\ell(x) - S(x)\| \leqslant r$. □

From above propositions, we conclude that for $\lambda > 0$ large enough, there are two symmetric solutions η_s, η_ℓ of (3.1), where η_s is near zero and η_ℓ is near $S(x)$.

3.2. Nonexistence of steady solutions for small λ

In the following, we show nonexistence of solutions of (3.1) for small $\lambda \geqslant 0$ with *positive forcing* $b(x) \geqslant 0$ but $b(x) \not\equiv 0$. Here, for the sake of convenience, $b(x)$ is assumed to have a compact support in $[-1, 1]$ with $b(x) > 0$ for $x \in (-1, 1)$. Then, we prove that (3.1) has no solution that approaches to zero as $x \to \pm\infty$ for $\lambda \geqslant 0$ near zero.

Proposition 3.3. *There exists a constant Λ_0 such that for $0 \leqslant \lambda < \Lambda_0$,* (3.1) *has no solutions that approach to zero at infinity.*

Proof. First, let us consider the case with $\lambda = 0$ in (3.1), which gives the equation

$$-(1/3)\eta_{xx} - (3/2)\eta^2 = b. \tag{3.8}$$

For $x \leqslant -1$, we have $b = 0$ and

$$-(1/3)\eta_{xx} - (3/2)\eta^2 = 0. \tag{3.9}$$

Multiply (3.9) by η_x and then integrate it from $-\infty$ to x,

$$-(1/6)(\eta_x)^2 - (1/2)\eta^3 = 0, \tag{3.10}$$

where $-\infty < x \leqslant -1$, which implies that $\eta \equiv 0$ or $\eta < 0$ for $x \leqslant -1$. The similar conclusion holds for $x \geqslant 1$. If $\eta < 0$ at some point in $(-\infty, -1] \cup [1, \infty)$, say, in $(-\infty, -1]$, then $\eta < 0$ for all $x \in (-\infty, -1]$ with $\eta(-1) < 0$ (otherwise, $\eta = \eta_x = 0$ at some point yields $\eta \equiv 0$), which implies by (3.9) that $\eta_x < 0$ as well since $\eta_x \to 0$ as $x \to -\infty$. Since $\eta \to 0$ as $x \to +\infty$ and $\eta_{xx} \leqslant 0$ for $x \in (-\infty, -1] \cup [1, \infty)$ with the solution smooth up to second order for all x, there must be a point $x_0 \in (-1, 1)$ such that $\eta_{xx}(x_0) > 0$, which is a contradiction to Eq. (3.8) at x_0 since $b(x_0) > 0$. Therefore, $\eta(x) \equiv 0$ for all $x \in (-\infty, -1] \cup [1, \infty)$.

By (3.8) again, it is deduced that

$$-(1/3)\eta_{xx} = (3/2)\eta^2 + b \geqslant 0.$$

Therefore, $\eta_{xx} \leqslant 0$ or η_x is nonincreasing for all x. But $\eta \not\equiv 0$ and $\eta = 0$ for $x \in (-\infty, -1] \cup [1, \infty)$, which is impossible for a function with a nonincreasing derivative. Thus, there is no solution of (3.1) for $\lambda = 0$.

If $\lambda > 0$, multiply (3.1) by η_x and integrate the result from $-\infty$ to x to have

$$-(1/6)(\eta_x)^2 - (1/2)\eta^3 + \lambda\eta^2 = \int_{-1}^{x} \eta_x b \,\mathrm{d}x. \tag{3.11}$$

If $x \leqslant -1$, then

$$-(1/6)(\eta_x)^2 = (1/2)\eta^3 - \lambda\eta^2 = (1/2)\eta^2(\eta - 2\lambda) \tag{3.12}$$

which gives $\eta \leqslant 2\lambda$ for all $x \in (-\infty, -1]$. By (3.3), it is easy to see that $\eta > 0$ for all $x \in R$. Hence, the solution $\eta(x)$ of (3.12) must satisfy $0 < \eta(x) \leqslant 2\lambda$ for all $x \in (-\infty, -1] \cup [1, \infty)$, which yields that as $\lambda \to 0$, $\eta(x), \eta_x(x) \to 0$ for all $x(-\infty, -1] \cup [1, \infty)$.

Claim. *Given any fixed $\Lambda < +\infty$, if $0 \leqslant \lambda \leqslant \Lambda$, the solutions of* (3.1) *are uniformly bounded for x in* $[-1, 1]$.

Proof of the claim. Write (3.1) as

$$-\frac{1}{3}\eta_{xx} = \frac{3}{2}\eta\left(\eta - \frac{4}{3}\lambda\right) + b(x). \tag{3.13}$$

First, note that $\eta > 0$ in $[-1, 1]$. If $\eta \leqslant (4\lambda/3)$, then $|\eta_{xx}| \leqslant (8/3)\lambda^2 + 3\max|b(x)|$. At $x = -1$, $\eta \leqslant 2\lambda$. By (3.10), $|\eta_x(-1)| \leqslant 24\lambda^3$. Thus, by the boundedness of η_{xx},

$$|\eta_x| \leqslant 24\lambda^3 + (16\lambda^2/3) + 6\max\big|b(x)\big| \tag{3.14}$$

in $[-1, 1]$ if $\eta \leqslant (4\lambda/3)$. For $\eta > (4\lambda/3)$, (3.13) implies that $\eta_{xx} < 0$, i.e. η_x is strictly decreasing. Thus, (3.14) holds for all $x \in [-1, 1]$, which yields the uniform boundedness of η for $x \in [-1, 1]$ with respect to $0 < \lambda \leqslant \Lambda$. The claim is proved. □

By the claim and (3.1), η is equi-continuous in $[-1, 1]$ with respect to λ with $0 < \lambda \leqslant \Lambda$. By Arzela–Ascoli theorem, there is a sequence $\lambda_j \to 0$ and $\eta_0(x) \in C[-1, 1]$ such that $\eta_{\lambda_i} j(x) \to \eta_0(x)$ in $C[-1, 1]$. Since $|\eta_{\lambda_j}(x)| \leqslant 2\lambda_j$ for $x \in (-\infty, -1] \cup [1, \infty)$, we can integrate (3.1) for $\eta_{\lambda_j}(x)$ twice to obtain

$$-(1/3)\eta(x) = \int_{-1}^{x}\int_{-1}^{s}\big(-2\lambda\eta(t) + (3/2)\eta^2(t) + b(t)\big)\,\mathrm{d}t\,\mathrm{d}s - (1/3)\eta_x(-1) + \eta(-1), \tag{3.15}$$

which gives that η_0 is twice differentiable and $\partial_x^i \eta_{\lambda_j}(x) \to \partial_x^i \eta_0(x)$ for $i = 1, 2$ and $x \in [-N, N]$ with $N > 1$. Thus, by letting $\lambda_j \to 0$ in (3.15), we obtain that η_0 satisfies (3.1) with $\lambda = 0$, which contradicts that there is no solution of (3.1) with $\lambda = 0$. The proof is completed. □

From Proposition 3.3, there exists a $\Lambda_0 > 0$ such that for any $0 \leqslant \lambda \leqslant \Lambda_0$, Eq. (3.1) has no solution which decays to zero at infinity. From Propositions 3.1, 3.2 and 3.3, it is deduced that there is a finite cut-off value λ_0 such that for $0 \leqslant \lambda < \lambda_0$ there are no solutions of (3.1) while there is a solution of (3.1) for $\lambda = \lambda_0$. Note that by using the same proof of the claim in the proof of Proposition 3.3, it can be shown that the set of λ for the existence of solutions of (3.1) is closed.

3.3. Numerical solutions

In this subsection, we use numerical computation to find symmetric solutions of (3.1) when $b(x)$ is given by $b(x) = R(1 - x^2)^{1/2}$ for $|x| \leqslant 1$ and $b(x) = 0$ for $|x| > 1$ where R is a given positive constant.

First, we find solutions for $|x| > 1$. In this region, $b(x) = 0$ and the solutions of (3.1) can be explicitly found, which are $\eta = 0$ or $\eta = 2\lambda\,\mathrm{sech}^2[(6\lambda)^{1/2}(x - x_0)/2]$ with a free constant x_0. Here, note that by (3.3), η must be positive. To find symmetric solutions in $|x| \leqslant 1$, we only have to calculate the solution of (3.1) for $-1 \leqslant x \leqslant 0$ subject to $\eta_x^2 = -3\eta^3 + 6\lambda\eta^2$ at $x = -1$ and $\eta_x = 0$ at $x = 0$ by varying the phase shift x_0, which in turn changes $\eta(-1) = 2\lambda\,\mathrm{sech}^2[(6\lambda)^{1/2}(-1 - x_0)/2]$. This problem is solved numerically using a shooting method and the numerical results are presented in Figs. 2 and 3. Fig. 2 shows the relationship between $\eta(0)$ and λ, where $R = 0.2, 0.5, 1.0$, and 2.0. Two typical solutions η_s and η_ℓ corresponding to $\lambda = 1.5$, $R = 1$ are show in Fig. 3. We note that the solution η_ℓ is a solution near $S(x)$ and the solution η_s is a solution near 0. From Fig. 2, it is seen that there are no solutions when $\lambda > 0$ small and for large λ there are two branches of symmetric solutions, one near zero and one near $S(x)$, which confirms the theoretical results presented in Propositions 3.1–3.3. The numerical results presented here were also obtained in [24].

4. Time dependent FKdV equation

In this section we study the solutions of the time-dependent FKdV equation (1.2) theoretically and numerically.

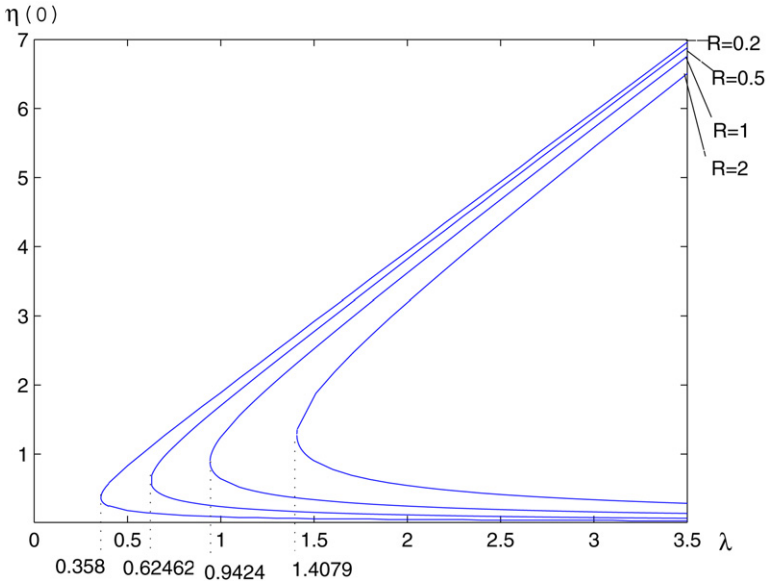

Fig. 2. The relation between λ and $\eta(0)$.

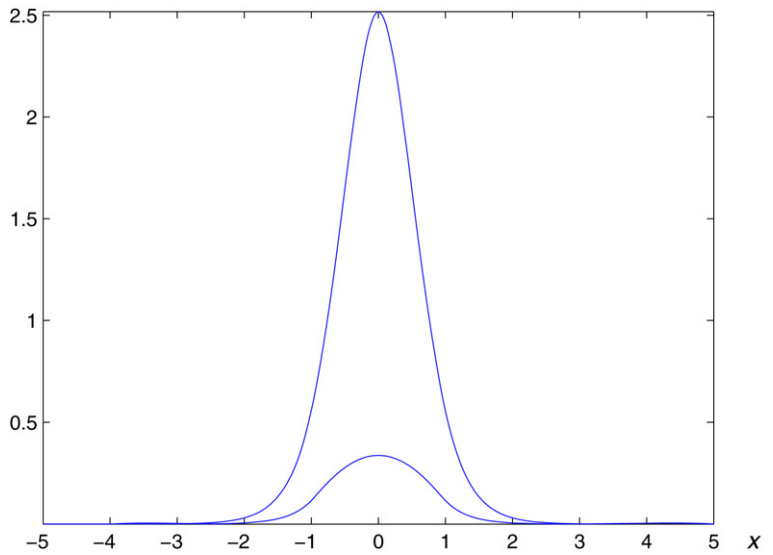

Fig. 3. Typical forms of solutions $\eta_\ell(x)$ and $\eta_s(x)$ for $\lambda = 1.5$.

4.1. Global well-posedness of initial value problem

In this subsection, we study (1.2) with initial condition

$$\eta(x, 0) = \eta_0(x) \tag{4.1}$$

and give the global existence of solution in the Sobolev space $H^1(R)$.

First, let us consider some conserved quantities of (1.2). Such conserved quantities have been obtained in [7,8]. For the sake of convenience, they are derived again here. Multiply both sides of (1.2) by η and integrate it from $-\infty$ to $+\infty$ to obtain

$$\int_{-\infty}^{\infty} (\eta^2)_t \, dx = \int_{-\infty}^{\infty} 2\eta b_x \, dx. \tag{4.2}$$

Then, multiply (1.2) by η_{xx} and η^2, respectively, and integrate results again to have

$$\int_{-\infty}^{\infty} \left(-\left((\eta_x)^2\right)_t + 3\eta^2\eta_{xxx}\right) dx = \int_{-\infty}^{\infty} 2\eta_{xx} b_x \, dx, \tag{4.3}$$

$$\int_{-\infty}^{\infty} \left((\eta^3)_t - \eta^2\eta_{xxx}\right) dx = \int_{-\infty}^{\infty} 3\eta^2 b_x \, dx. \tag{4.4}$$

Multiply (4.4) by 3 and add it to (4.3), which gives

$$\int_{-\infty}^{\infty} \left(-\left((\eta_x)^2\right)_t + 3(\eta^3)_t\right) dx = \int_{-\infty}^{\infty} (2\eta_{xx} b_x + 9\eta^2 b_x) \, dx,$$

or

$$\int_{-\infty}^{\infty} \left(-\left((\eta_x)^2/6\right)_t + (\eta^3/2)_t\right) dx = \int_{-\infty}^{\infty} \left(-(1/3)\eta_{xxx} b - (3/2)(\eta^2)_x b\right) dx. \tag{4.5}$$

Then, multiply (4.2) by $-\lambda$ and add the result to (4.5) to yield

$$\begin{aligned}\int_{-\infty}^{\infty} \left(-\left((\eta_x)^2/6\right) + (\eta^3/2) - \lambda\eta^2\right)_t dx &= \int_{-\infty}^{\infty} \left(-(1/3)\eta_{xxx} b - (3/2)(\eta^2)_x b + 2\lambda\eta_x b\right) dx \\ &= \int_{-\infty}^{\infty} (-\eta_t + b_x) b \, dx = \int_{-\infty}^{\infty} (-\eta b)_t \, dx\end{aligned}$$

which gives a conserved quantity

$$\int_{-\infty}^{\infty} \left(\left((\eta_x)^2/6\right) - (\eta^3/2) + \lambda\eta^2 - \eta b\right) dx. \tag{4.6}$$

Now, we discuss the initial value problem of (1.2) and (4.1). For given initial data (4.1), the initial value problem with $b = 0$ has been well studied in $H^s(R)$ space for $s > -3/4$ [17]. Here, we only concentrate on integer s with $s \geqslant 1$. The local well-posedness of (1.2) and (4.1) can be easily obtained using classical contraction mapping principle similar to the one used for the case $b = 0$ [2], as long as b is compacted supported and smooth enough. Then, the global well-posedness can be derived if one can establish *a priori* global $H^s(R)$-estimates for smooth solution η of (1.2). Here, we only consider the case with $s = 1$.

The global estimate for L^2 space can be obtained directly from (4.2) and Gronwall inequality. From (4.2), if we let $u_1(t) = \|\eta(\cdot, t)\|_{L^2(R)}$, then

$$\frac{d}{dt} u_1^2(t) \leqslant 2u_1(t) \int_{-\infty}^{\infty} |b_x| \, dx$$

which gives

$$u_1(t) \leqslant u_1(0) + t \int_{-\infty}^{\infty} |b_x| \, dx. \tag{4.7}$$

Then, the global estimate of η in $H^1(R)$ is obtained using the conserved quantity (4.6). Here, we note that

$$\|\eta^2\|_{L^\infty(R)} \leqslant \|\eta\|_{L^2(R)}\|\eta_x\|_{L^2(R)} \tag{4.8}$$

and the generalized Schwartz inequality gives

$$\begin{aligned}\left|\int_{-\infty}^{\infty}\eta^3\,dx\right| &\leqslant \|\eta\|_{L^\infty}\|\eta\|^2_{L^2(R)} \leqslant \big(\|\eta\|_{L^2}/\delta^{1/5}\big)^{5/2}\big(\delta\|\eta_x\|_{L^2}\big)^{1/2}\\ &\leqslant (1/4)\delta^2\|\eta_x\|^2_{L^2} + (3/4)\big(\|\eta\|_{L^2}/\delta^{1/5}\big)^{10/3}.\end{aligned} \tag{4.9}$$

Thus, for $\delta > 0$, (4.6) gives a bound on $\|\eta_x\|_{L^2}$ using (4.7) and (4.9), which yields the global well-posedness of the initial problem. Therefore, for arbitrary initial condition $\eta_0(x)$ in $H^1(R)$, the solution of (1.2) with (4.1) in $H^1(R)$ exists for $t \in [0, +\infty)$.

4.2. *Lyaponov stability of $\eta_s(x)$ for large $\lambda > 0$*

As was pointed out in Section 3, two symmetric time-independent solitary-wave-like solutions η_s and η_ℓ exist if λ is greater than a cut-off value of λ. In this subsection we show that η_s is stable in the Lyaponov sense for large $\lambda > 0$.

Proposition 4.1. *If $\lambda > \sqrt{3\|b(x)\|/2} = s_0$, then the solution $\eta_s(x)$ obtained from Proposition* 3.1 *is stable with respect to* (1.2) *in the space $H^1(R)$.*

Proof. Consider (1.2) and let $\eta(x,t) = \eta_s(x) + u(x,t)$. The equation of $u(x,t)$ is

$$u_t - (1/3)u_{xxx} - (3/2)\big((u + 2\eta_s)u\big)_x + 2\lambda u_x = 0 \tag{4.10}$$

with the initial condition $u(x,0) = u_0(x)$. If we assume that $u_0(x) \in H^1(R)$, by the global well-posedness of the problem, the solution $u(x,t)$ exists for all $t \in [0, +\infty)$. By the conserved quantities in (4.2) and (4.6) and Eq. (3.1) that η_s satisfies, we have

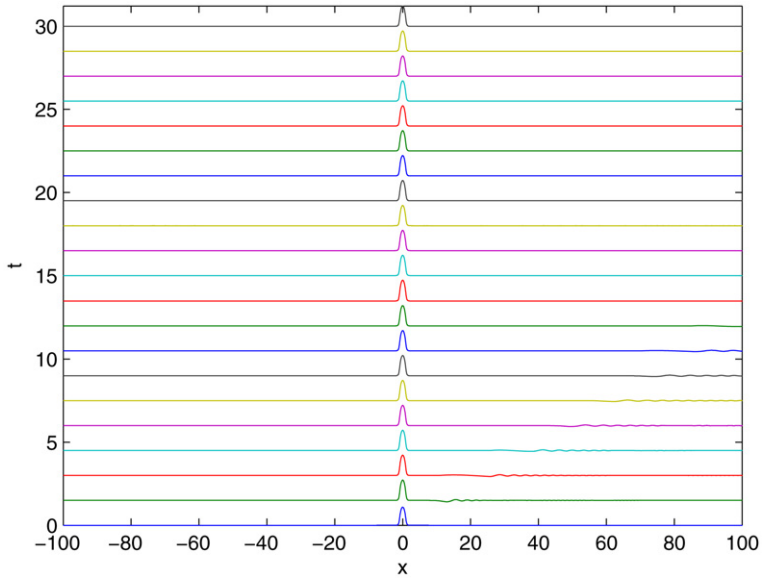

Fig. 4. Time evolution of the solution of (1.2) with initial condition near $\eta_s(x)$.

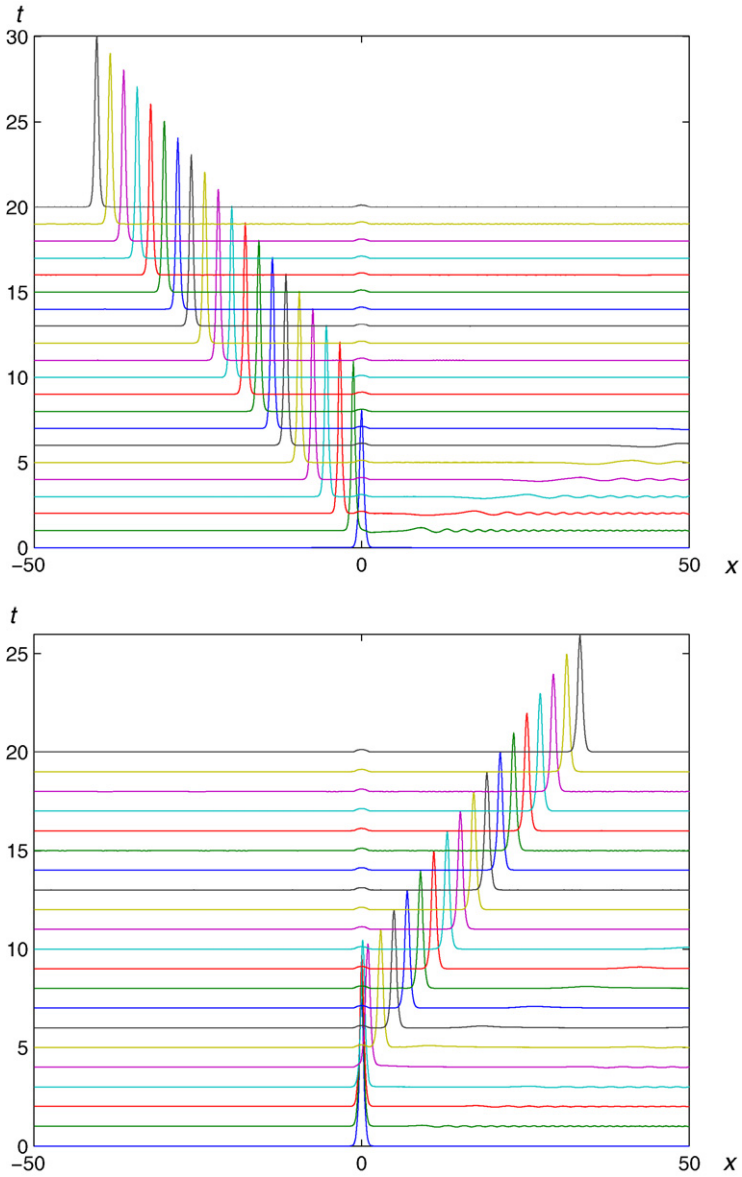

Fig. 5. Time evolution of the solution of (1.2) with initial condition near $\eta_\ell(x)$.

$$\int_{-\infty}^{\infty} \left(\left(u_x^2(x,t)/6\right) - \left(\left(u(x,t)\right)^3/2\right) - \left(3\left(u(x,t)\right)^2\eta_s/2\right) + \lambda\left(u(x,t)\right)^2\right) dx$$
$$= \int_{-\infty}^{\infty} \left(\left(u_{0x}^2(x)/6\right) - \left(\left(u_0(x)\right)^3/2\right) - \left(3\left(u_0(x)\right)^2\eta_s/2\right) + \lambda\left(u_0(x)\right)^2\right) dx.$$

From (3.3), if $\lambda > s_0$, then $|\eta_s(x)| \leqslant \sqrt{2\|b(x)\|/3}$. Using (4.9) for the function u, we have

$$\left| \int_{-\infty}^{\infty} (u^3/2)\, dx \right| \leqslant (1/8)\delta^2 \|u_x\|_{L^2}^2 + (3/8)\left(\|u\|_{L^2}/\delta^{1/5}\right)^{10/3}$$

which for $\delta = 1$ gives

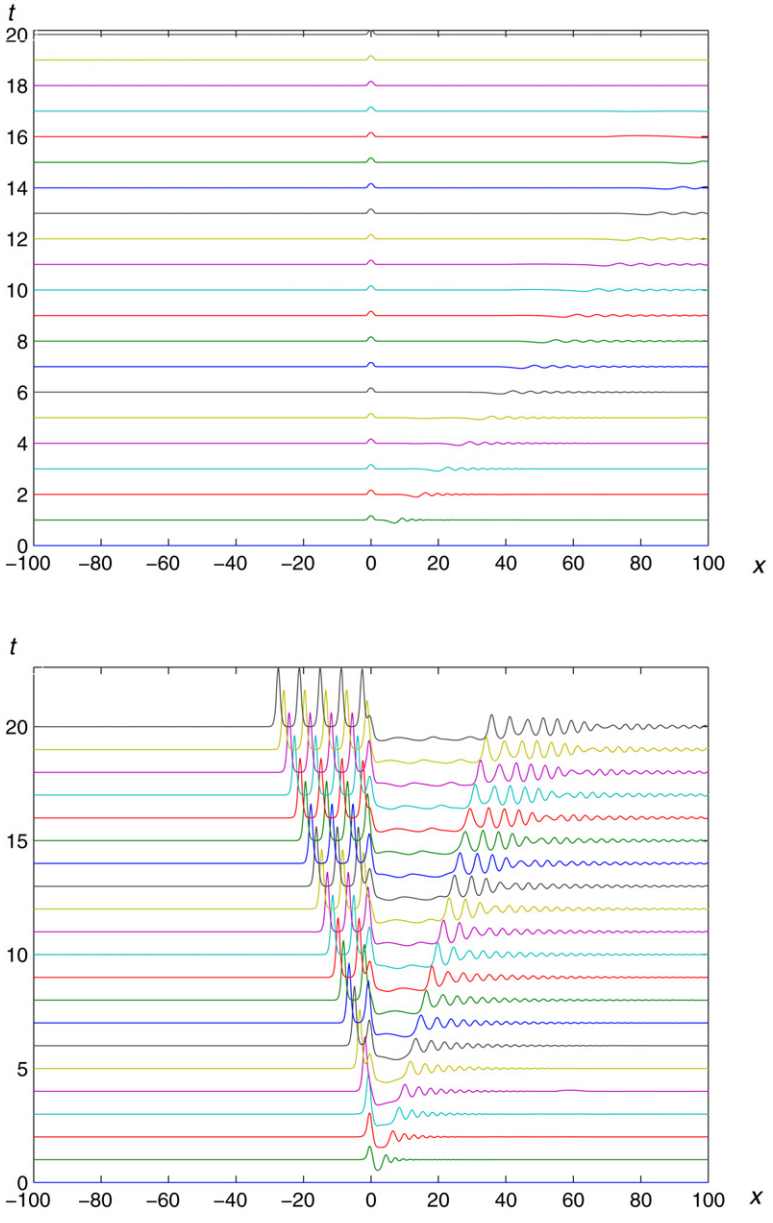

Fig. 6. Time evolution of the solution of (1.2) with $\eta(x,0) \equiv 0$: $\lambda = 3$ and $\lambda = 0.5$.

$$\int_{-\infty}^{\infty} \left(\left((1/6) - (1/8)\right)u_x^2(x,t) + \left(\lambda - (3\eta_s/2) - (3/8)\left(\|u\|_{L^2}\right)^{4/3}\right)u^2(x,t)\,dx$$

$$\leqslant \int_{-\infty}^{\infty} \left(\left(\left(u_{0x}(x)\right)^2/6\right) - \left(\left(u_0(x)\right)^3/2\right) - \left(3\left(u_0(x)\right)^2\eta_s/2\right) + \lambda\left(u_0(x)\right)^2 dx \tag{4.11}$$

and yields the Lyaponov stability of η_s in $H^1(R)$. Its proof is given by contradiction. If η_s is not stable, then there is a small $\epsilon_0 > 0$ with $\lambda - s_0 > (3/8)\epsilon_0^{4/3}$ such that there exists a sequence of initial data $u_{0n}(x)$ with

$$\lim_{n\to\infty} \left\|u_{0n}(x)\right\|_{H^1(R)} = 0 \quad \text{and} \quad \left\|u_n(x,t_n)\right\|_{H^1(R)} = \epsilon_0$$

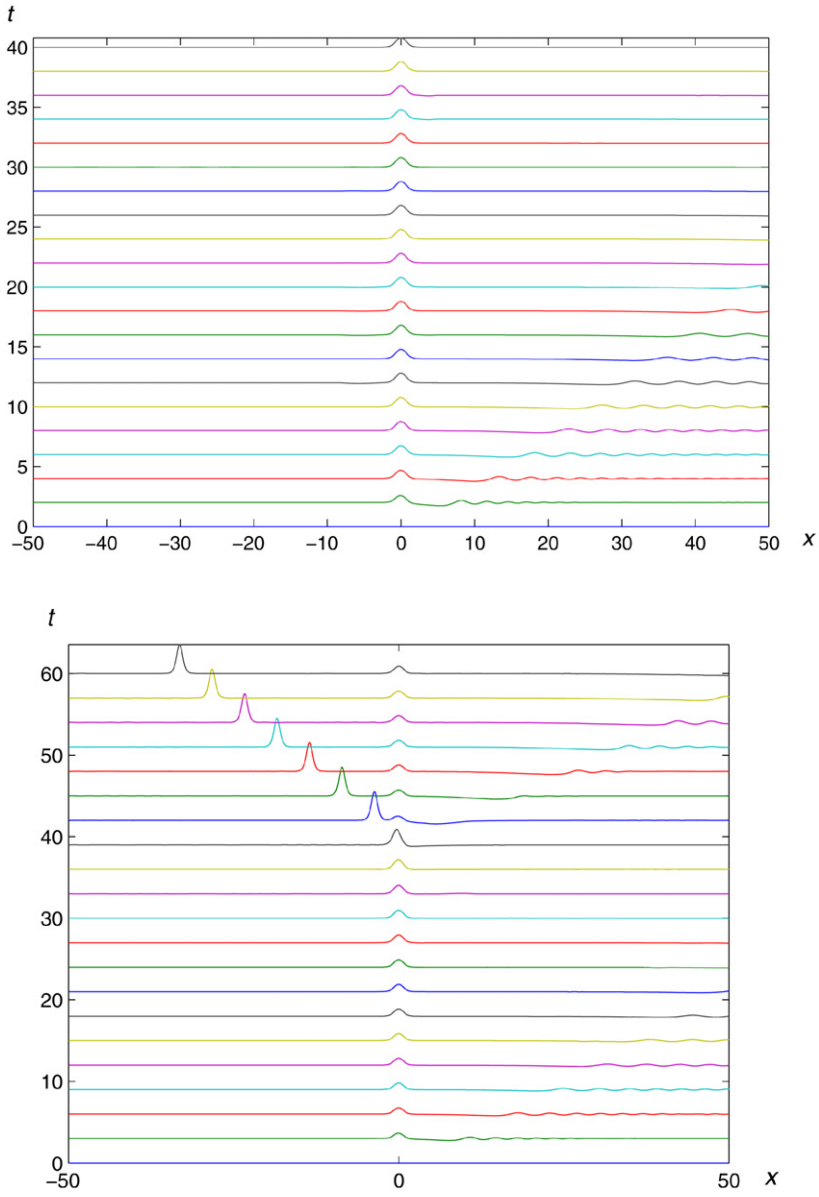

Fig. 7. Time evolution of $\eta(x,0) \equiv 0$ for $\lambda = 0.95$ and $\lambda = 0.94$, respectively.

for some $t_n > 0$, where $u_n(x,t)$ is the solution of (1.2) with initial condition $u_{0n}(x)$. Apply (4.11) to $u_n(x,t)$ and obtain

$$\begin{aligned}
&\int_{-\infty}^{\infty} \big(\big((1/6)-(1/8)\big)u_{nx}^2(x,t_n) + \big(\lambda - s_0 - (3/8)\epsilon_0^{4/3}\big)u_n^2(x,t_n)\big)\,dx \\
&\leqslant \int_{-\infty}^{\infty} \big(\big((1/6)-(1/8)\big)u_{nx}^2(x,t_n) + \big(\lambda - (3\eta_s/2) - (3/8)\big(\|u_n(\cdot,t_n)\|_{L^2}\big)^{4/3}\big)u_n^2(x,t_n)\big)\,dx \\
&\leqslant \int_{-\infty}^{\infty} \big(\big(u_{0nx}^2(x)/6\big) - \big(\big(u_{0n}(x)\big)^3/2\big) - \big(3\big(u_{0n}(x)\big)^2\eta_s/2\big) + \lambda\big(u_{0n}(x)\big)^2\big)\,dx, \qquad (4.12)
\end{aligned}$$

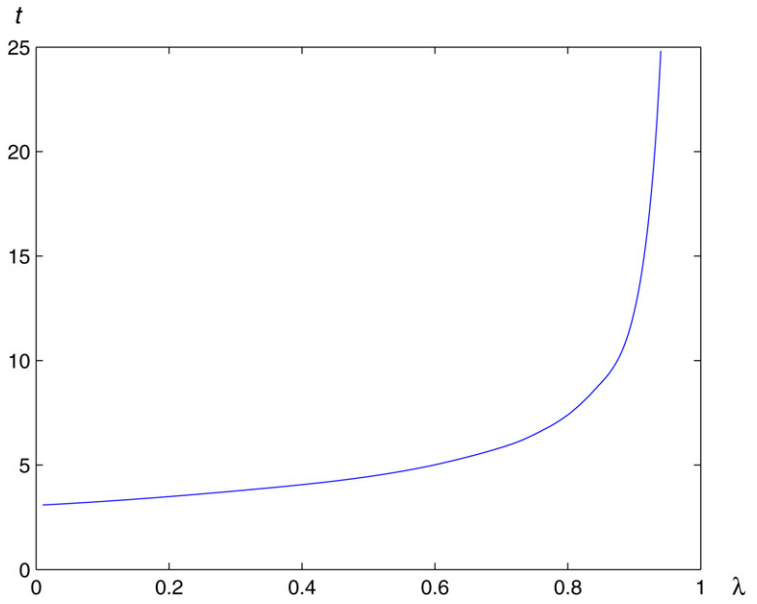

Fig. 8. The relation between λ and the time period T.

where $|\eta_s(x)| \leqslant \sqrt{2\|b(x)\|/3}$ and $\|u_n(x,t_n)\|_{L^2} \leqslant \epsilon_0$ have been used. By the assumption on $u_n(x,t)$ and $\lambda - s_0 > (3/8)\epsilon_0^{4/3}$, the left side of (4.12) is greater than $C_0\epsilon_0^2$ and the right side goes to zero as $n \to +\infty$, which is a contradiction. Thus, the zero solution of (4.10) is stable or η_s of (3.2) is stable for (1.2) if $\lambda > s_0$. □

4.3. Numerical computation

In this subsection we investigate numerically the behavior of solutions of (1.2) for different initial conditions (4.1) with a fixed forcing $b(x)$. The forcing term $b(x)$ in (1.2) is chosen as $b(x) = (1-x^2)^{1/2}$ for $|x| \leqslant 1$ and $b(x) = 0$ for $|x| > 1$. Therefore, from Section 3, there is a cut-off value $\lambda_0 \sim 0.9424$ for λ such that there are two symmetric steady solutions of (1.2) for each $\lambda > \lambda_0$ and no steady solutions for $0 \leqslant \lambda < \lambda_0$. For the numerical method of finding the solution of the IVP (1.2) and (4.1), a generalized Crank–Nicolson scheme is used to discretize the temporal variable and the discretized fast Fourier transform method is used for the spatial variable. Thus, the periodic boundary conditions are used for the spatial variable. The detailed discussion on this method can be found in the book by Trefethen [27]. The interval considered in the numerical computation for spatial variable is $-600 \leqslant x \leqslant 600$. The time and space steps are 10^{-4} and 10^{-2}, respectively. The software package MATLAB has been used for the computation of the fast Fourier transforms.

4.3.1. Numerical stability of steady solutions

As was pointed out in Section 3, if λ is greater than a cut-off value λ_0, there are two symmetric solutions η_s and η_ℓ of (3.1). Here, the stability and instability of these solutions are studied numerically. When the initial data η_0 of (4.1) is close to either η_s or η_ℓ, the behavior of solution of (1.2) with η_0 is investigated as time evolves.

First, let us consider the stability of η_s. In Subsection 4.2, we know that for $\lambda > s_0$, η_s is stable. The numerical result of (1.2) for this case is obtained when the initial condition (4.1) is taken as η_s plus 10% noise, and is given in Fig. 4. Fig. 4 shows the time evolution of the solution when $\lambda = 3.0$. As is shown in the figure, small dispersive waves appear and move to down steam. As time tends to infinity, the solution converges to η_s. Here, the actual numerical computation is accomplished for $-600 \leqslant x \leqslant 600$. The same phenomena happen in all values of λ for which η_s exists.

Then, we study the instability of η_ℓ for (1.2). The initial condition is chosen as η_ℓ plus 5% or minus 5% perturbation. Fig. 5 shows the time evolution of solution of (1.2) in this case for $\lambda = 3.0$. When the total perturbation in $L^2(R)$ is positive, the amplitude of the solution becomes larger as time is increasing and a traveling solitary-wave is generated

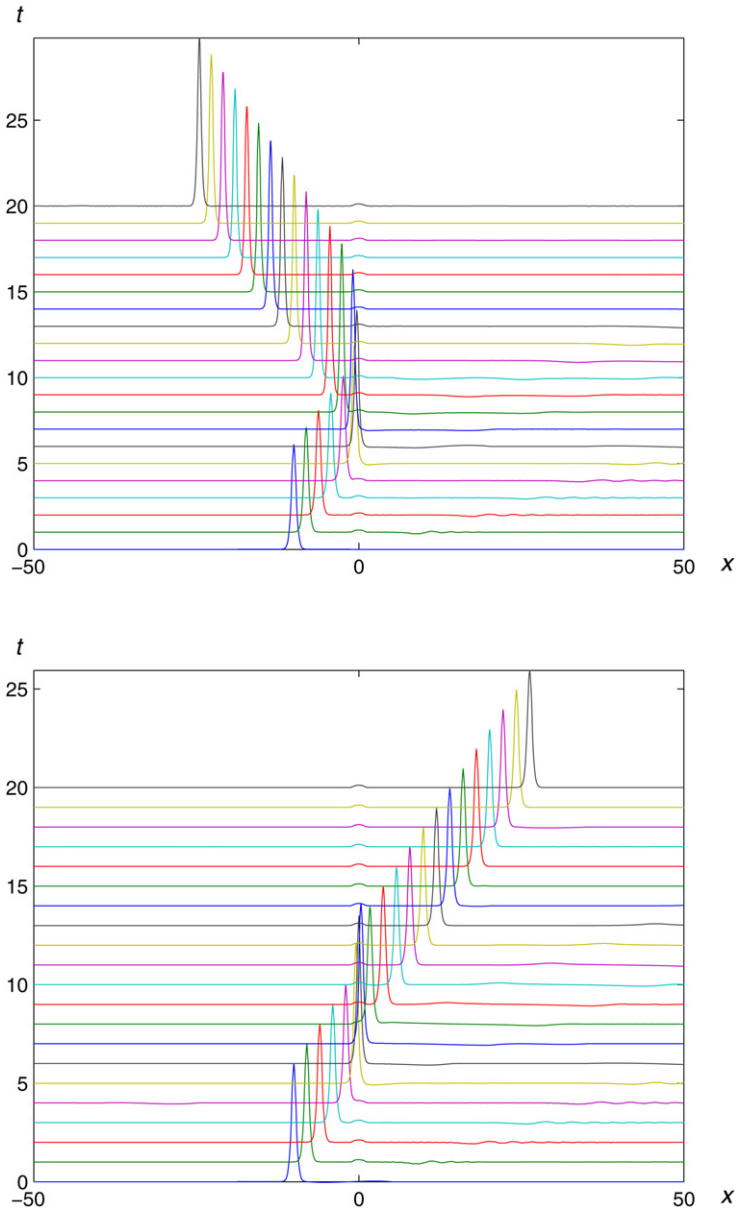

Fig. 9. Time evolution of traveling solitary wave with $\lambda = 4$, $x_0 = -10$ with $c = 1.9$ and $c = 2$, respectively.

after a certain time and moves to the upstream. Small dispersive waves with small amplitude appear and propagate to the downstream. As time evolves, both traveling solitary-wave and small oscillatory waves propagate apart from the bump and the steady solution η_s appears above the bump, which is stable. Moreover, if the total perturbation in $L^2(R)$ is negative, the same phenomenon holds except that the traveling solitary wave moves to the downstream. Such phenomena happen to all cases of λ for which η_ℓ exists. Thus, for each $\lambda > \lambda_0$, a traveling solitary-wave is generated after a certain time and moves to upstream or downstream and oscillatory dispersive waves with small amplitude appear and propagate to downstream.

Again, we note that the actual numerical computation is accomplished for $-600 \leqslant x \leqslant 600$ even the graph is shown only for $-100 \leqslant x \leqslant 100$ or $-50 \leqslant x \leqslant 50$. In [29,15], they studied the numerical stability of η_ℓ by using $\eta_\ell(x)$ as the initial condition and taking the numerical noise as the perturbation.

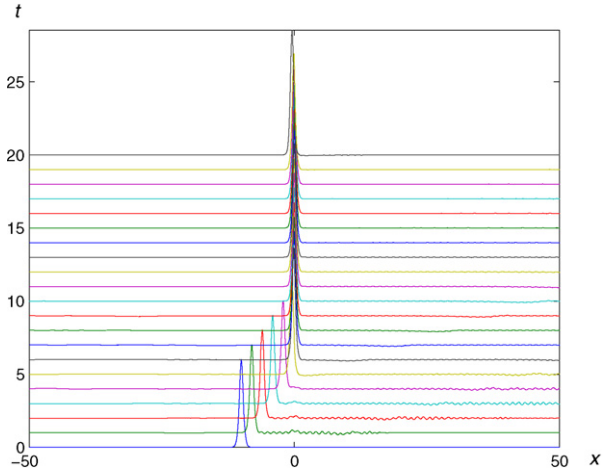

Fig. 10. Time evolution of traveling solitary wave for $\lambda = 4$, $x_0 = -10$ when $c = 1.9863264835$.

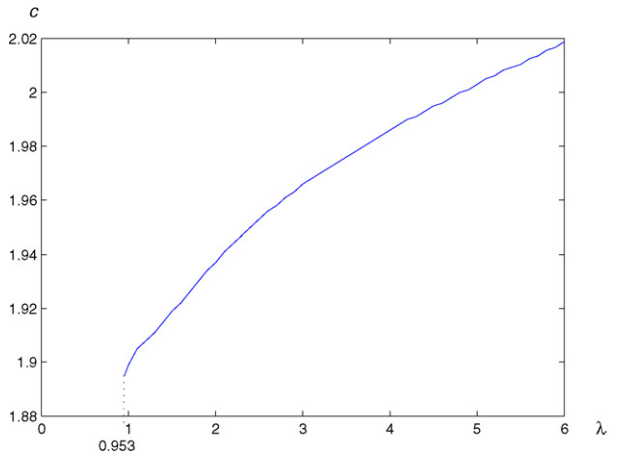

Fig. 11. The relation between λ and the critical speed c_0 of c.

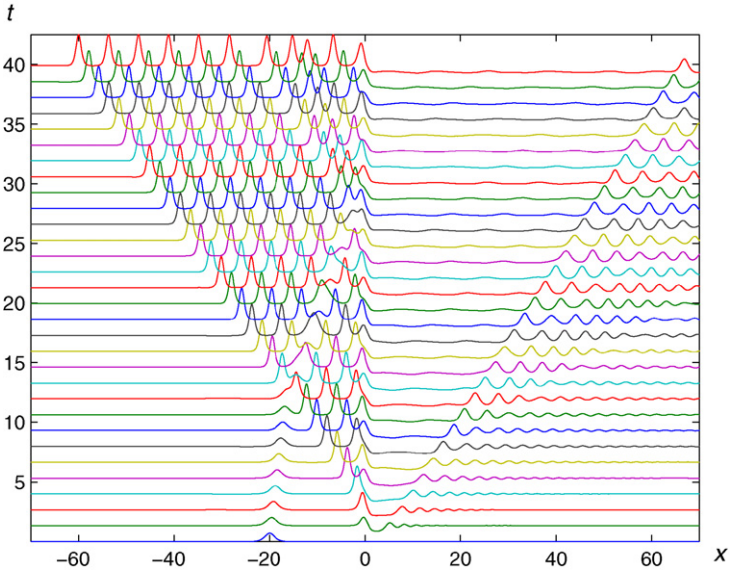

Fig. 12. Time evolution of solution with $\eta(x,0) = (7/10)\,\mathrm{sech}^2(\sqrt{21/10}(x-20)/2)$ for $\lambda = 0.5$, $x_0 = -20$, and $c = 0.3$.

4.3.2. Numerical solutions with zero initial condition

Here, numerical solutions of (1.2) with initial condition $\eta_0 \equiv 0$ are discussed. The behaviors of the solutions are different for different values of λ. For $\lambda \geqslant \lambda_0 = 0.9424$, the solutions converge to η_s as time goes to infinity. The numerical result is given in Fig. 6. Fig. 6 shows the time evolution of the solution η of (1.2) for $\lambda = 3.0$. For $0 \leqslant \lambda < \lambda_0$, which is the case that there are no steady solutions of (1.2), a trail of solitary-waves are generated ahead of the bump and moving to the upstream, which is also shown in Fig. 6. It shows the time evolution of the solution η for (1.2) with $\lambda = 0.5$. The similar numerical solutions for $\lambda < \lambda_0$ have been calculated in [1,11,20,29].

The graphs for the time evolution of solutions η of (1.2) with $\lambda = 0.94$ (slightly less than λ_0) and $\lambda = 0.95$ (slightly greater than λ_0) are given in Fig. 7. It is seen that when λ is less than λ_0 but near λ_0, the time period T for generating one solitary wave ahead of the bump becomes large. As $\lambda \to \lambda_0^-$, $T \to +\infty$. There is no solitary wave generated when $\lambda \geqslant \lambda_0$. In Fig. 8, we show the relation between λ and T when λ is between 0 and the cut-off value λ_0.

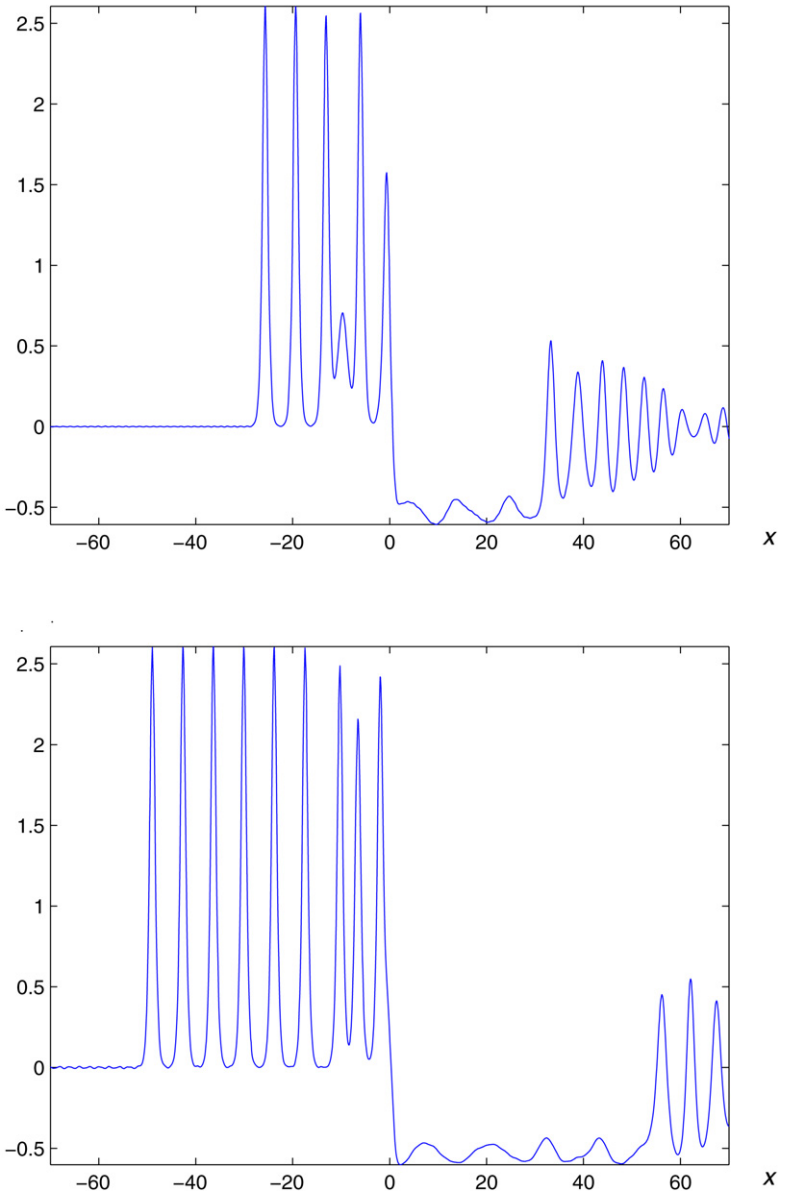

Fig. 13. Snapshot of Fig. 12 when $t = 18.5$ and $t = 33.5$.

4.3.3. Solutions with traveling solitary waves as initial conditions

In this subsection, we study the solutions of (1.2) with initial conditions (4.1) chosen as

$$\eta(x,0) = \eta_0(x) = S_{c,x_0}(x,t)|_{t=0} = (2\lambda - c)\,\mathrm{sech}^2\big(\sqrt{3(2\lambda - c)}(x - x_0 - ct)/2\big)|_{t=0} \tag{4.13}$$

where $S_{c,x_0}(x,t)$ is a solitary-wave solution of the KdV equation

$$u_t - (1/3)u_{xxx} - 3uu_x + 2\lambda u_x = 0, \tag{4.14}$$

c stands for the traveling velocity of the wave, and x_0 is a phase shift, which is chosen as reasonably large, that is, the initial solitary wave is far away from the bump. Here, we are interested in how the bump affects the motion of the solitary waves.

First, let us consider the case with $x_0 < 0$ and $c > 0$, i.e. a solitary wave is coming from the upstream and moving to the downstream. In this case, we need $c < 2\lambda$.

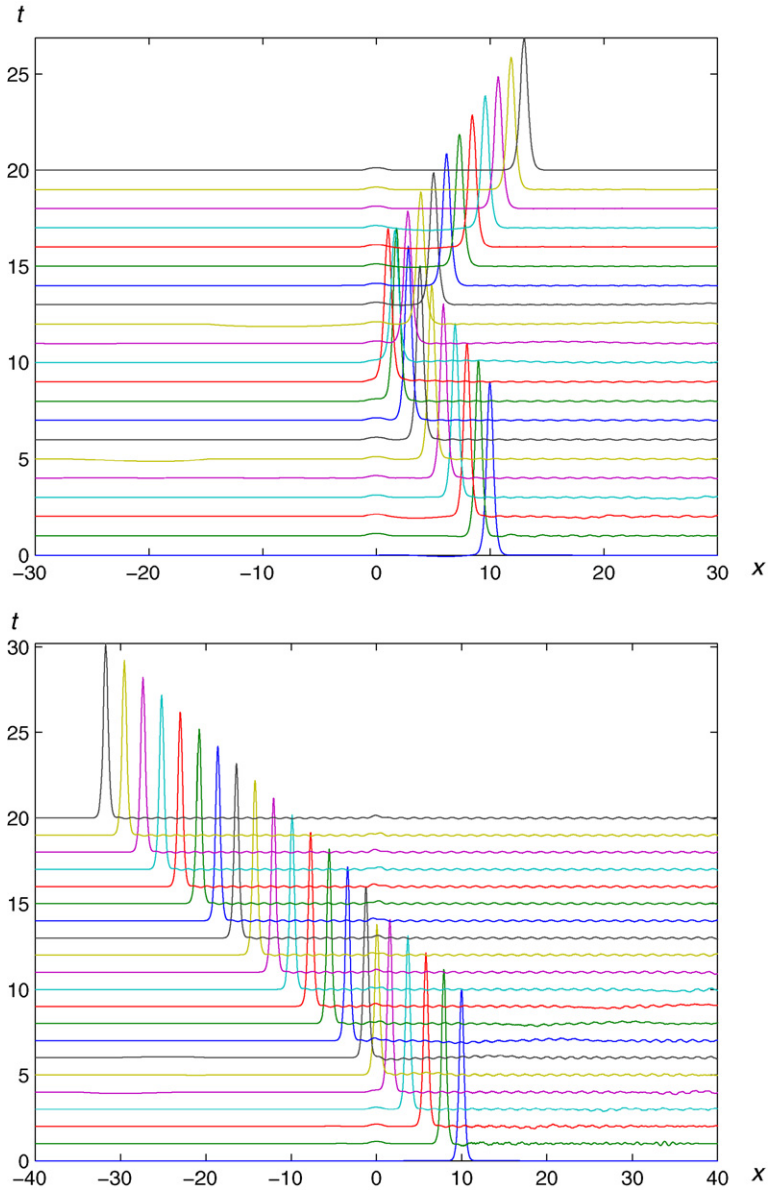

Fig. 14. Time evolution of traveling solitary waves with $\lambda = 4$, $x_0 = 10$ when $c = -1, -2$, respectively.

In the case that $\lambda > \lambda_0 = 0.9424$, we note that η_s is stable. When a traveling solitary wave is moving towards the bump and reaches to the bump, the wave corresponding to the solution of (1.2) either reflects itself by the bump and moves to the upstream or passes over the bump and moves to the downstream, depending upon the speeds of the initial solitary waves. Numerical examples are given in Fig. 9. In Fig. 9, we choose $\lambda = 4$, phase shift $x_0 = -10$, and the speed of the solitary wave $c = 1.9$ and $c = 2$, respectively. In the case of $c = 1.9$, the traveling solitary wave moves to the right at the beginning and changes its traveling direction as it reaches $x = -1$, which is the left end of the support of $b(x)$. Small oscillatory waves are generated and move toward the downstream and a steady wave appears over the support of the $b(x)$, which is η_s. For the case of $c = 2$, the solitary wave passes over the support of $b(x)$, small oscillatory waves appear and move to the downstream, and a steady wave again appears over the support of $b(x)$.

By a more detailed numerical study, we can show that for $\lambda = 4$, the upstream solitary wave changes its traveling direction if $c \lesssim 1.9863264835$ and it passes over the bump if $c \gtrsim 1.9863264835$. Fig. 10 shows that near the critical value of c, the solitary wave moves over the bump, stays there for a quite long time and becomes more like a steady

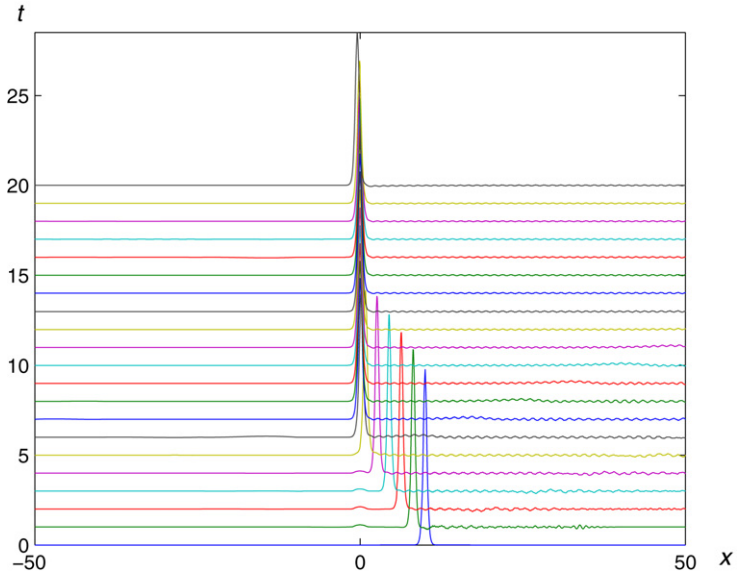

Fig. 15. Time evolution of traveling solitary wave for $\lambda = 4$, $x_0 = 10$ when $c = -1.7657159668$.

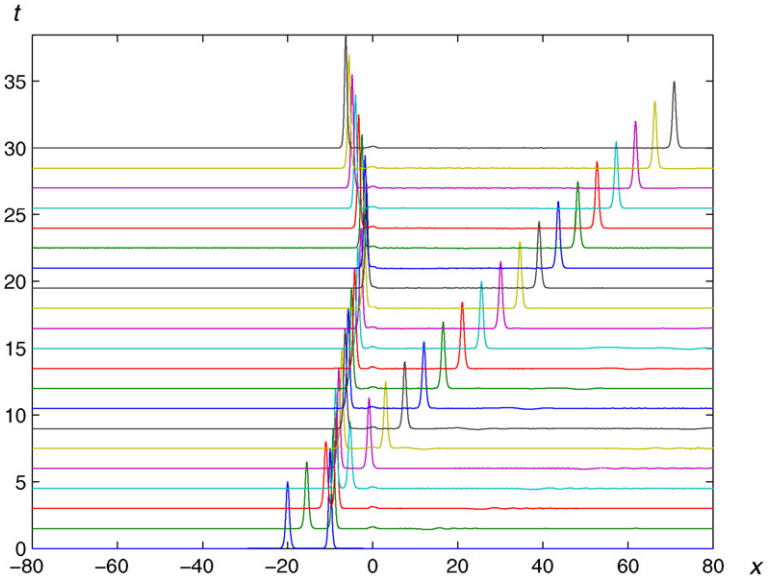

Fig. 16. Time evolution of two-soliton solution for $\lambda = 4$ with $x_0 = -20, -10$ and $c = 3, 0.5$.

solution $\eta_\ell(x)$. It will eventually move away from the bump because of the numerical noise and the instability of η_ℓ. In Fig. 11, we show the relation between λ and the critical speed c_0. If the speed of the solitary wave is greater than c_0, then the surface wave passes over the bump, while it reflects from the bump if the speed is less than c_0.

For $\lambda < \lambda_0 = 0.9424$, it is known in Subsection 4.3.2 that for the zero initial condition, there exist waves generated periodically ahead of the bump. If a traveling solitary-wave is initially placed far upstream and moving towards the bump, it interacts with the periodic wave generated due to the bump as time evolves. The interaction is elastic and more like soliton interaction. Here, we are cautious on the difference between soliton and solitary waves since we are not sure that the waves generated by the bump are really solitons. Fig. 12 gives the numerical solution of (1.2) using the initial condition (4.13) by taking $\lambda = 0.5 < \lambda_0$, $x_0 = -20$, and $c = 0.3$ so that $\eta(x, 0) = (7/10)\,\mathrm{sech}^2(\sqrt{21/10}(x +$

$20 - 3t/10)/2)|_{t=0}$. Fig. 13 shows the snapshots of Fig. 12 when $t = 18.5$ (before the reflection) and 33.5 (after reflection), respectively.

Similar phenomena happen when the initial solitary wave moves to the bump from the downstream (that is, $c < 0$ and $x_0 > 0$ in the initial condition (4.13)). Again, there is a critical speed for $|c|$. If $|c|$ is less than the critical speed, then the solitary wave corresponding to the solution of (1.2) changes its traveling direction as it reaches the right end of the support of $b(x)$. If $|c|$ is great than the critical number, the solitary wave passes over the support of $b(x)$ and continues moving to the upstream. Fig. 14 shows the time evolution of the traveling solitary wave with $\lambda = 4$, $x_0 = 10$ for $c = -1$ and $c = -2$, respectively. Fig. 15 gives the evolution of the traveling solitary wave with $\lambda = 4$, $x_0 = 10$ and c near the critical speed $c_0 = -1.7657159668$. Again, when c is near c_0, the traveling wave stays over the bump for a long time and resembles the steady solution η_ℓ.

Moreover, we consider the initial condition (4.1) to be taken as a two-soliton solution of the KdV equation (1.1) placed far upstream. In Fig. 16, we approximately let the speeds of the faster and slower solitary waves be $c = 3$ and $c = 0.5$, respectively, and the centers of the faster and slower solitary waves be chosen as $x_0 = -20$ and $x_0 = -10$, respectively. Fig. 16 shows that the slower one changes its traveling direction as it reaches the support of $b(x)$ and the faster one passes over the support of $b(x)$.

Acknowledgement

The research reported here was supported by MIC, Korea, under the ITRC support program. SMS was partially supported by the National Science Foundation. JWC appreciates the support of Korea University, Korea. The authors are grateful for the comments and suggestions given by the reviewers.

References

[1] T.R. Akylas, On the excitation of long nonlinear water waves by a moving pressure distribution, J. Fluid Mech. 141 (1984) 455–466.
[2] J.L. Bona, B.-Y. Zhang, The initial-value problem for the forced Korteweg–de Vries equation, Proc. Roy. Soc. Edinburgh A 126 (1996) 571–598.
[3] J. Boussinesq, Théorie de l'intumescence liquide appelée onde solitaire ou de translation se propageant dans un canal rectangulair, C. R. Acad. Sci. Paris 72 (1871) 755–759.
[4] J. Boussinesq, Théorie générale des mouvements qui sont propagés dans un canal rectangulaire horizontal, C. R. Acad. Sci. Paris 73 (1871) 256–260.
[5] J. Boussinesq, Théorie des ondes et des remous qui se propagent le long d'un canal rectangulaire horizontal, en communiquant au liquide contenu dans ce canal des vitesses sensiblement pareilles de la surface au fond, J. Math. Pures Appl. 17 (1872) 55–108.
[6] J. Boussinesq, Essai sur la théorie des eaux courantes, Mémoires présentés par divers savants á l'Académie des Sciences Inst. France (séries 2) 23 (1877) 1–680.
[7] R. Camassa, T.Y. Wu, Stability of some stationary solutions for the forced kdv equation, Physica D 51 (1991) 295–307.
[8] R. Camassa, T.Y. Wu, Stability of forced steady solitary waves, Philos. Trans. Roy. Soc. London Ser. A 337 (1991) 429–466.
[9] J.W. Choi, Symmetric current of a two layer fluid with free surface over an elliptic obstruction, J. Korean Math. Soc. 34 (1997) 119–133.
[10] J.W. Choi, S.M. Sun, M.C. Shen, Steady capillary-gravity waves on the interface of two-layer fluid over an obstruction-forced modified K-dV equation, J. Eng. Math. 28 (1994) 193–210.
[11] S.L. Cole, Transient waves produced by a flow past a bump, Wave Motion 7 (1985) 579–587.
[12] F. Dias, J.M. Vanden-Broeck, Two layer hydraulic falls over an obstacle, Eur. J. Mech. B Fluids 23 (2004) 879–898.
[13] L.K. Forbes, Critical free surface flow over a semi-circular obstruction, J. Eng. Math. 22 (1988) 3–13.
[14] L.K. Forbes, L.W. Schwartz, Free surface flow over a semi-circular obstruction, J. Fluid. Mech. 144 (1982) 299–314.
[15] L. Gong, S.P. Shen, Multiple supercritical solitary wave solutions of the stationary forced KdV equation and their stability, SIAM J. Appl. Math. 54 (1994) 1268–1290.
[16] R.H.J. Grimshaw, N. Smyth, Resonant flow of a stratified fluid over topography, J. Fluid Mech. 169 (1986) 429–464.
[17] C.E. Kenig, G. Ponce, L. Vega, A bilinear estimate with applications to the KdV equation, J. Amer. Math. Soc. 9 (1996) 573–603.
[18] D.J. Korteweg, G. de Vries, On the change of form of long waves advancing in a rectangular canal, and on a new type of long stationary waves, Phil. Mag. (Ser. 5) 39 (1895) 422–443.
[19] S.J. Lee, G.T. Yates, T.Y. Wu, Experiments and analyses of upstream-advancing solitary waves generated by moving disturbances, J. Fluid Mech. 199 (1989) 569–593.
[20] C.C. Mei, Radiation of solitons by slender bodies advancing in a shallow channel, J. Fluid Mech. 162 (1986) 53–67.
[21] J.W. Miles, Stationary, transcritical channel flows, J. Fluid Mech. 162 (1986) 489–499.
[22] L. Rayleigh, On waves, Phil. Mag. (Ser. 5) 1 (1876) 257–279.
[23] J.S. Russell, Report on waves, in: Report of the 14th Meeting of the British Association for the Advancement of Science, London, U.K., John Murray, 1844, pp. 311–390.
[24] S.P. Shen, M.C. Shen, S.M. Sun, A model equation for steady surface waves over a bump, J. Eng. Math. 23 (1989) 315–323.

[25] J.J. Stoker, Water Waves: The Mathematical Theory with Applications, Pure and Applied Mathematics, vol. IV, Interscience Publishers, Inc., New York, 1957.
[26] S.M. Sun, Existence of a generalized solitary wave solution for water with positive Bond number less than 1/3, J. Math. Anal. Appl. 156 (1991) 471–504.
[27] L.N. Trefethen, Spectral Methods in MATLAB, SIAM, Philadelphia, PA, 2000.
[28] J.M. Vanden Broeck, Free surface flow over a semi-circular obstruction in a channel, Phys. Fluids 30 (1987) 2315–2317.
[29] T.Y. Wu, Generation of upstream advancing solitons by moving disturbances, J. Fluid Mech. 184 (1987) 75–99.
[30] D.M. Wu, T.Y. Wu, Three-dimensional nonlinear long waves due to moving surface pressure, Proc. 14th Sump. Naval Hydrodyn. 1982, 103–125.